Available online at www.sciencedirect.com

ScienceDirect

Advances in Space Research 56 (2015) 1400–1412

ADVANCES IN SPACE RESEARCH (a COSPAR publication)

www.elsevier.com/locate/asr

Anomalous changes in ionospheric TEC during an earthquake event of 13–14 April 2010 in the Chinese sector

Malini Aggarwal

Indian Institute of Geomagnetism, Navi Mumbai, Mumbai, India

Received 26 March 2015; received in revised form 7 July 2015; accepted 8 July 2015
Available online 14 July 2015

Abstract

The earth's ionosphere is considered susceptible to the seismic effects and the detection of such ionospheric perturbations associated with the earthquake has become a challenge for the short-term prediction of earthquakes. In this paper, an investigation of the changes in the ionospheric behavior is reported which may be associated with M 6.9 and its aftershock of 6.1 magnitude earthquakes at Qinghai station (geog. 33.19°N, 96.75°E, geom. 23.90°N, 169.98°E) which occurred on 13 April (~23:49 UT, 06:19 LT on 14 Apr) and 14 April 2010 (~01:25 UT, 06:55 LT) respectively. The observations are made using ionospheric total electron content (TEC) obtained from 10 available IGS stations in the Chinese and 2 in the Indian sector to detect seismo-ionospheric anomalies if they exists. We found anomalous depletions in the ionospheric regions ~3–4 days (on 10 April 2010) up to ~4 TECU before the earthquake over stations close to the epicenter (<1700 km). The anomalous changes in the ionosphere are observed firstly over a distant station (wuhn, ~0800–1600 UT) during afternoon to midnight hours and few hours later over the near-by stations to the epicentre in the nighttime (~1500–2300 UT, ~2100–0500 LT). Our results from the case study suggest that these anomalies in ionospheric TEC may be the possible seismo-ionospheric signatures for the considered earthquake in the Tibetian plateau region.

Keywords: Earthquake; Total electron content (TEC); Ionosphere

1. Introduction

The seismo-ionospheric coupling has opened up a new important challenge for the scientific community and it is taking a lot more attention in the last three decades (e.g., Pulinets et al. 2002; Plotkin 2003; Ruzhin et al. 2002; Stein and Okal 2005; Tronin et al. 2002 and many more). There are a number of reported evidences which shows that the electromagnetic phenomenons are possibly associated with the seismic activities (Hayakawa and Fujinawa 1994; Calais and Minster, 1995; Hayakawa and Molchanov 2002 and many more). The first recorded anomalous signals in the time series of the ionospheric total electron content (TEC) were obtained by Calais and Minster (1995) using the permanent GPS network operated in southern California in the frequency band of 10–3 min after Northridge earthquake which occurred on 17 Jan, 1994 (Mw = 6.7). The signal frequency and propagation phase velocity (300–600 m/s) were in agreement with the results of numerical simulation for acoustic gravity waves (AGW) caused by a rapid uplift and subsidence of the Earth' surface during the earthquake. The velocity was determined as a ratio of the distance from earthquake's epicenter to Sub-Ionospheric Point (SIP) to the time delay of perturbations received at the corresponding SIP.

The large earthquakes are reported to be often preceded by signals of different nature: electric, magnetic, electromagnetic, luminous etc (Gokhberg et al. 1982; Parrot and Lefeuvre, 1985). The possible mechanism for the generation of electromagnetic waves in the lithosphere was

E-mail address: asmalini@rediffmail.com

http://dx.doi.org/10.1016/j.asr.2015.07.007
0273-1177/

identified through the microfracturing process of rocks responsible for geo-electric and geomagnetic field anomalies as well as the development of strong ionospheric perturbations preceding strong earthquakes. Some of these signals can propagate up to the ionosphere and generate changes in the various ionospheric parameters like electron and ion temperatures, electron densities, total electron content (TEC), virtual height (hmF2) etc (e.g. Akhoondzadeh et al., 2010; Sharma et al., 2013). The mechanism of ionospheric anomalies includes direct coupling between the earth's surface (lithosphere) and the lower ionosphere through electric current (Pulinets et al. 2000), and triggering of AGW by gas releases or thermal anomalies (Gokhberg et al., 1994; Molchanov and Hayakawa, 2001).

The recent ground-based and satellite observations have also shown the possibilities of generation of ionospheric disturbances by earthquake preparation processes. The ground based measurements may/may not be available at the same location where the seismic event might have occurred. To overcome this shortcoming, the satellite measurements which may have a vast coverage of the seismic zones of the Earth along with other sources of information may be regarded as a suitable means for the earthquake studies. Many papers and special monographs have come out on satellite observations of electromagnetic and ionospheric perturbations associated with seismic activity (Hayakawa and Molchanov, 2002; Pulinets and Boyarchuk, 2004). Gokhberg et al. (1983) studied the variability of local plasma density and temperatures measured onboard AE-C and ISIS-2 satellites. Pulinets et al. (2003) used the data of ground-based ionosondes and topside sounding from onboard Alouette-2 and Intercosmos-19 satellites together with the local plasma measurements onboard the AE-C satellite to classify the main features of ionospheric variations associated with pre-seismic activities. The seismic-ionospheric disturbances are found to be weakly generated several days before the first shock away from the epicenter. Sharma et al. (2013) using SROSS C2 satellite data at ~500 km mainly from the Indian sector observed enhancement in the temperatures of electron by 1.2–1.5 and for ions by 1.1–1.3 times respectively during the seismic events. Recently, Akhoondzadeh et al. (2010) using plasma analyzer and Langmuir probe onboard DEMETER satellite and GPS measurements found a good agreement between the different parameters of the ionosphere (electron density, electron temperature, ion density and TEC) in the detection of pre-seismic anomalies. They observed different anomalous deviations prior to earthquakes from event to event with the amplitude variability depending on the magnitude of the earthquake. Various researchers have also reported observations of seismo-ionospheric variabilities with both positive (enhancement) and negative (depletion) effects on electron density (Pulinets et al., 1994 and many more). In the recent times, the high resolution measurements of GPS (Global Positioning System) – TEC have also made a significant contribution to the understanding of seismo-ionospheric variabilies. Liu et al. (2004a) using TEC data for 20 major earthquakes in Taiwan during September 1999-December 2002 statistically described the temporal parameters of the seismo-ionospheric precursors and found a decrease during 1–5 days (80% cases) prior to the earthquake. Moreover, Liu et al. (2009) reported that the anomalous TEC reductions which appeared 3–5 days before 17 events of 6.3 earthquakes in China region from May 1, 1998 to April 30, 2008 and the result was also found consistent with the case study of the 2008 Wenchuan earthquake (M7.9). In addition, an extreme increase of TEC for all the analyzed period is recorded in the afternoon of 3 days before the earthquake. Devi et al. (2008) showed that electric field generated during earthquake preparatory processes has a strong effect in shaping the TEC profiles of the northern crest of the equatorial anomaly. Recently Astafyeva et al. (2013) found from 11 seismic events, that the amplitude of coseismic TEC variations in the near-field is larger after strong earthquakes, and the stronger earthquakes ($M > 7.9$) are in general characterized by a longer negative phase in coseismic perturbations. Xia et al. (2011) studied the pre-earthquake ionospheric anomalies during three earthquakes and found that the upper and lower anomalies in GPS-TEC occur 2–9 days prior to earthquakes and occur in 30 degree in latitude around the epicenters during the afternoon and evening periods. Sharma et al. (2010) observed unusual enhancements of ionospheric foF2 and TEC during three earthquakes in China which appeared 1–4 days before the main shock and especially during 1100–1700 LT.

In order to gain a robust insight into the ionospheric precursors of earthquake, our investigation is aimed to shed new light on the complex behavior of the ionosphere during the earthquake event which occurred at Qinghai, China (33.19°N, 96.75°E) on 13 and its aftershocks on 14 April 2010 ((M~6.9, 23:50 UT and ~6.1, 01:25 UT) respectively by carrying out the detailed analysis of changes in the ionospheric TEC behavior over near-by and far-away (<3000 km) distances from the epicenter of the earthquake. For this study, we obtained TEC measurements from 10 available IGS stations from China and 2 stations in the Indian sector and examined the anomalies using the method employed by Liu et al. (2009). Recently Astafyeva and Heki (2011) and Pundhir et al. (2014) also adopted same technique as that by Liu et al. (2009). Pundhir et al. (2014) found anomalous enhancements and depletions in TEC 1–9 days before the occurrence of main shock for an event of 16 April 2013 (Mw = 7.8).

2. The earthquake description

The strong earthquake of magnitude 6.9 occurred on 13 April, 2010 around 23:49:37 UT (14 April 2010 around 06:19:37 LT) at the epicenter (geog. 33.19°N, 96.75°E, geom. 23.90°N, 169.98°E), with shallow depth ~13.8 km in the Southern Qinghai, China. The published report says (http://earthquake.usgs.gov/earthquakes/eqinthenews/

2010/us2010vacp/#summary) that at least 2,698 people were killed, 270 missing, 12,135 injured and 15,000 buildings damaged in the Yushu area. It was felt intense (IV) at Lhasa, Qiaotou and Xining stations with weaker intensity (II) at Baojishan, Lanzhou and Urumqi. The tremors were also felt (II) at Thimphu (Bhutan), Dibrugarh (India), Kathmandu (Nepal) and Chiang Mai (Thailand). This earthquake occurred as a result of strike-slip faulting in the tectonically complex region of the eastern Tibetan Plateau and is one of the largest known historic earthquakes within several hundred kilometers of its location. This earthquake occurred several hundred kilometers north of the convergent India: Eurasia plate boundary, where the Indian Plate is moving northwards with respect to Eurasia at a rate of approx. 46 mm/yr. This convergence drives the uplift of the Himalaya Mountains, at a rate of approximately 10 mm/yr, and the Tibetan Plateau, which is an extremely broad region of thickened and uplifted crust sitting above 4.5–5 km.

The various characteristics of earthquake event and its aftershock (14 April 2010, 6.1 magnitude around 01:26:16 UT) were obtained from the United State Geological Survey (USGS) website (www.earthquake.usgs.gov.in). The details of these earthquakes which include the day of its occurrence, location, depths, magnitudes, time of occurrence in UT and LT at epicenter is described in Table 1. The radius of the earthquake preparatory zone in the lithosphere is obtained using the expression, $R = 10\text{\^{}}(0.43\ \mathrm{M})$, where M is the magnitude of the earthquake event (Dobrovolsky et al. 1979).

3. Data set and analysis technique

To examine the interplanetary conditions during study period, the significant parameters like Interplanetary magnetic field (IMF Bz, nT) in geocentric-solar-magnetospheric (GSM) coordinates, electric field associated with IMF (E, mV/m) in 1-min resolution, 3-hourly Kp and hourly Dst indices are obtained from the OMNI website. The hourly EUV flux in 0.1–50 nm band is obtained by CELIAS/SEM experiment onboard the SOHO spacecraft. To investigate the spatial and temporal irregular behavior of the ionosphere before and during the earthquake event, the total electron content (TEC) is obtained by the GPS (sampling rate ~30 s) using 10 IGS stations over the Chinese sector. (TEC being defined as the total number of electrons in the ionosphere from the GPS satellite height (~20,000 km) to the receiver in a unit cross-sectional area, 1 TECU = 10^{16} el/m^2). To make a comparison away from the epicenter, the ionospheric GPS-TEC over 2 IGS stations in the Indian sub-continent is also determined. The vertical TEC is obtained from the slant TEC by using the method of a thin layer approximation under the assumption that the ionosphere is a single layer at a height of 350 km (Klobuchar, 1986). In our analysis, only the satellite measurements with elevation angle higher than 20° are selected to minimize the time shift and avoid unwanted errors due to multipath. Fig. 1(a) illustrates the location of the epicenter (starred) and the relative distance of the considered GPS receivers (dotted). The circle represents the preparatory or influence zone of the earthquake of radius ~930 km. The three stations (bjfs, chan and urum) are in further north of Qinghai whereas others are toward the equator side. The bang is a lower-latitudinal whereas urum and chan are higher mid-latitude stations. The Table 2 lists the coordinates of IGS stations with the increasing distance from the epicenter considered in our study. The distance from epicenter to the IGS station is obtained by using the station coordinates in the Haversine formula. Out of these stations, we found that Lhasa (lhaz) lies in the preparatory zone of earthquake whereas Kunming (kunm) is just at the boundary. The Bangalore (bang) station in Indian continent is farthest (>2968 km) from Qinghai.

In order to detect abnormal signals in the GPS-TEC, we performed the data analysis as by Liu et al. (2009) using hourly vertical TEC for the ionosphere above the IGS stations (Table 2). This method is gaining significance in determining the precursors and has been adopted by many researchers e.g. Astafyeva and Heki (2011) and Pundhir et al. (2014). We determined the hourly median, M for the successive previous 15 days of TEC and found the deviation between the observed TEC on the 16th day (Obs TEC) and the computed median, M. To obtain quantitative information about the deviation, we obtained the associated lower (first) quartile (LQ) and upper (third) quartile (UQ) for the same universal time (UT) of TEC estimates over each station. It is to be noted that under the assumption of a normal distribution with mean (m) and standard deviation (s) for the TEC, the expected values of M and LQ or UQ are m and 1.34 s, respectively (Klotz and Johnson, 1983). Then we set the isolated TEC anomalies by defining the lower bound (LB) and upper bound (UB) defined as $LB = M - 1.5(M\text{-}LQ)$ and $UB = M + 1.5(UQ\text{-}M)$

Table 1
List the various characteristics of earthquake event as obtained by the USGS website.

S.No	Epicentre location	Coor	Date	Time, UT	Time, LT (UT + 06:30 h)	Mag	Depth, km	Radius of preparation zone
1	Qinghai, China	33.19°N, 96.75°E	13-Apr-10	23:49:37	6:19:37	6.9	13.8	930 km
2	Qinghai, China	33.15°N, 96.49°E	14-Apr-10	1:25:16	7:55:16	6.1	12.2	420 km

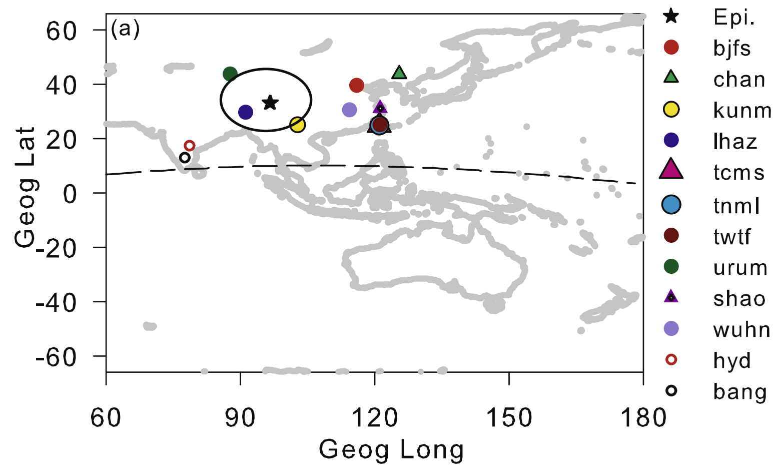

Fig. 1. Locations of the epicenter (Qinghai, star) and IGS stations (circle and triangle symbol) considered in the China and Indian sub-continent. The bigger circle represents the preparatory area and the dashed horizontal line the magnetic-equator.

Table 2
Lists the various IGS stations used in the study with their locations, distance from the epicenter and relative LT. Note: Lhasa is in the radius of preparation zone of earthquake.

S. No.	IGS-station	Station ID	Lat (°N)	Long (°E)	Country	Distance from epicentre, km	LT, hh:mm
1	Lhasa	lhaz	29.65	91.1	China	664	UT + 06:00
2	Kunming	kunm	25.02	102.79	China	1080	UT + 06:50
3	Urumqi	urum	43.8	87.6	China	1422	UT + 05:50
4	Wuhan	wuhn	30.53	114.35	P.R China	1687	UT + 07:35
5	Fangshan	bjfs	39.6	115.89	China	1851	UT + 07:40
6	Sheshan	shao	31.9	121.2	China	2308	UT + 08:00
7	Hsinchu	tcms	24.79	120.98	Rep of China	2527	UT + 08:00
8	Hsinchu	tnml	24.79	120.98	Rep of China	2527	UT + 08:00
9	Hyderabad	hyd	17.41	78.55	India	2527	UT + 05:10
10	Taoyuan	twtf	24.95	121.16	Rep of China	2535	UT + 08:00
11	Changchun	chan	43.79	125.44	China	2743	UT + 08:20
12	Bangalore	bang	13.02	77.57	India	2968	UT + 05:10

respectively. Here, the probability of a new TEC in the interval (LB, UB) is approximately 65% (Liu et al. 2009). The median together with the associated LB and UB then provide references for the TEC variations on the 16th day. Thus when an observed TEC on the 16th day is higher or lower than its previous 15-day-based median by UB or LB, we declare an upper or lower abnormal TEC signal. Thus the median represents the undisturbed background TEC value, whereas negative or positive deviations indicate reduction or enhancement of TEC, respectively. According to the Liu et al.'s method, possible earthquakes related perturbations are detected if the observed TEC fall out of either the lower or upper bound, and the confidence level for the seismic signals is about 80–85% (Liu et al. 2000, 2001 and 2004a). As the TEC time resolution is 1 h, there are 24 data points available per day. If consecutively more than one third (8/24) of the upper or lower abnormal signals appear in one day, and the observed TEC is higher (lower) than the associated UB (LB), we may then declare as the upper (lower) anomalous day.

4. Results and discussion

The earth's ionosphere is subjected to numerous influences, from both above as well as below due to the variation in solar activity, geomagnetic activity, meteorological events, and anthropogenic effects. The ionosphere also exhibits normal day-to-day, seasonal and diurnal variations making it difficult to clearly identify possible pre-seismic ionospheric anomalies as it changes the ionospheric parameters, such as TEC, on a regional scale (Afraimovich and Astafyeva, 2008). Hence we firstly looked into the prevailing background conditions during our study period. The Fig. 2 represents the variations of solar EUV flux, (0.1–50 nm), interplanetary magnetic field, Bz, its associated electric field, Ey and magnetic indices on the ground, Kp and Dst indices during 1–20 April 2010. A moderate geomagnetic storm was produced during 5–7 Apr caused by a solar filament burst coming to the magnetosphere and accompanied by a coronal mass ejection (CME). An interplanetary shock wave was detected on

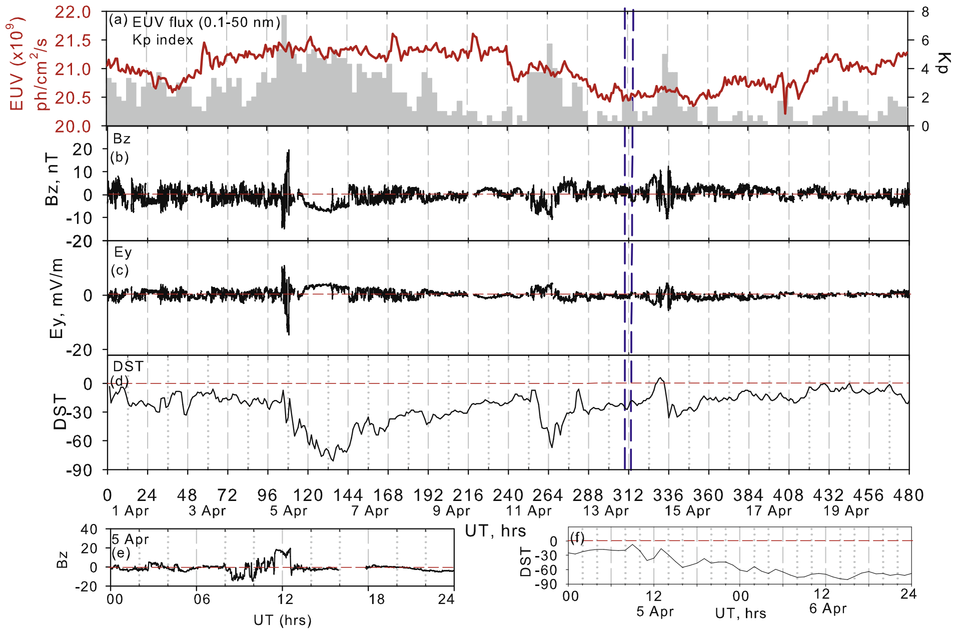

Fig. 2. Variability of background conditions of solar and interplanetary parameters (a) EUV flux and Kp indices (b) interplanetary magnetic field, Bz (c) east–west component of electric field, Ey and (d) DST indices during 1–20 April 2010 respectively. The two bottom plots represent the enlarged version of variations of (e) Bz on 5 Apr and (f) DST on 5 and 6 Apr 2010 respectively. The two vertical lines show the time of earthquake and its aftershock respectively.

the Earth on 5 Apr around 0830 UT as a sudden commencement (SC) of magnetic storm. It was the first notable geomagnetic storm of solar cycle 24. A sudden increase in the solar wind velocity from 500 km/s (before 0730 UT) to 700 km/s is observed around ~0800 UT in ~30 min duration. Then a further increase to maximum 800 km/s is observed around ~1400 UT which remained higher (>600 km/s) and gradually decelerated on the next day. At the same time, when solar wind velocity began increasing, the Bz turned southward and around 0800 UT was maximum to -14nT and then became highly northward around 0930 UT and then was fluctuating between north and southward directions. The associated Ey also turned eastward (~10 mV/m) when Bz turned southward. The Kp index reached a peak value of ~7.7 between 0900–1200 UT on 5 Apr. The Dst min (~ −81 nT) occurred on 6 Apr around 1500 UT. This magnetic storm began on the background of preceding geomagnetic perturbations with Kp up to ~4, lower values of the Dst index and the IMF, Bz component and a rather high solar wind velocity (~500 km/s). Despite being a relatively moderate storm as determined by the Dst index, it nevertheless had some devastating space weather impacts, including the malfunction of the Galaxy 15 communication satellite (at ~35,785 km) (Allen, 2010) and widespread GPS scintillations ranging from the Arctic to Antarctic (Prikryl et al. 2011; Kinrade et al. 2012).

Another weaker storm occurred on 11–12 Apr with Dst min ~ −67 nT around 0200 UT on 12 Apr. This storm is produced when the solar wind velocity enhanced from 360 (~1230 UT) to 460 km/s (~1500 UT) and with the turning of IMF, Bz to southward (around 1500 UT for more than 5 h, minimum ~ −7 nT) on 11 Apr. The Kp index became high (~5.7) during 0000–0300 UT on 12 Apr. This storm has produced the aurora Borealis in Shetland and Aurora Australis (http://www.sanap.ac.za/sanap_sanae/sanae_newsletters/S49%20Newsletter%20April%202010.pdf) on 12 Apr as reported.

The Fig. 3 represents the contours of observed TEC variabilities in the ionosphere and plasmasphere and its deviations from the median (Del TEC = M-Obs TEC) with respect to UT over each station during our study period of 1–20 Apr. The positive (negative) values of Del TEC indicate the lower (higher) measurements of observed TEC from the median respectively. Note here that the local time (LT) is different at stations and is already mentioned in Table 2. The TEC comprises of electron densities in the D, E and F layer of the ionosphere but main contribution is from the F-layer. The well known diurnal pattern of TEC exhibits a steady increase during early morning hours when the photoelectron begins and becomes maximum during noon time and then decreases due to the competitive effects of absence of photo-ionization and recombination of electrons with neutrals and ions respectively. It is well known that in the F region, the production rate of electron density depends on the atomic oxygen concentration [O] whereas the loss rate depends mainly on the molecular nitrogen concentration [N_2] with some contribution from molecular oxygen [O_2]. In Fig. 3, the observed TEC is minimum (⩽5 TECU) throughout the nighttime at all stations and start increasing during early morning hours. The rate of increase of TEC and the magnitude of noon-time TEC

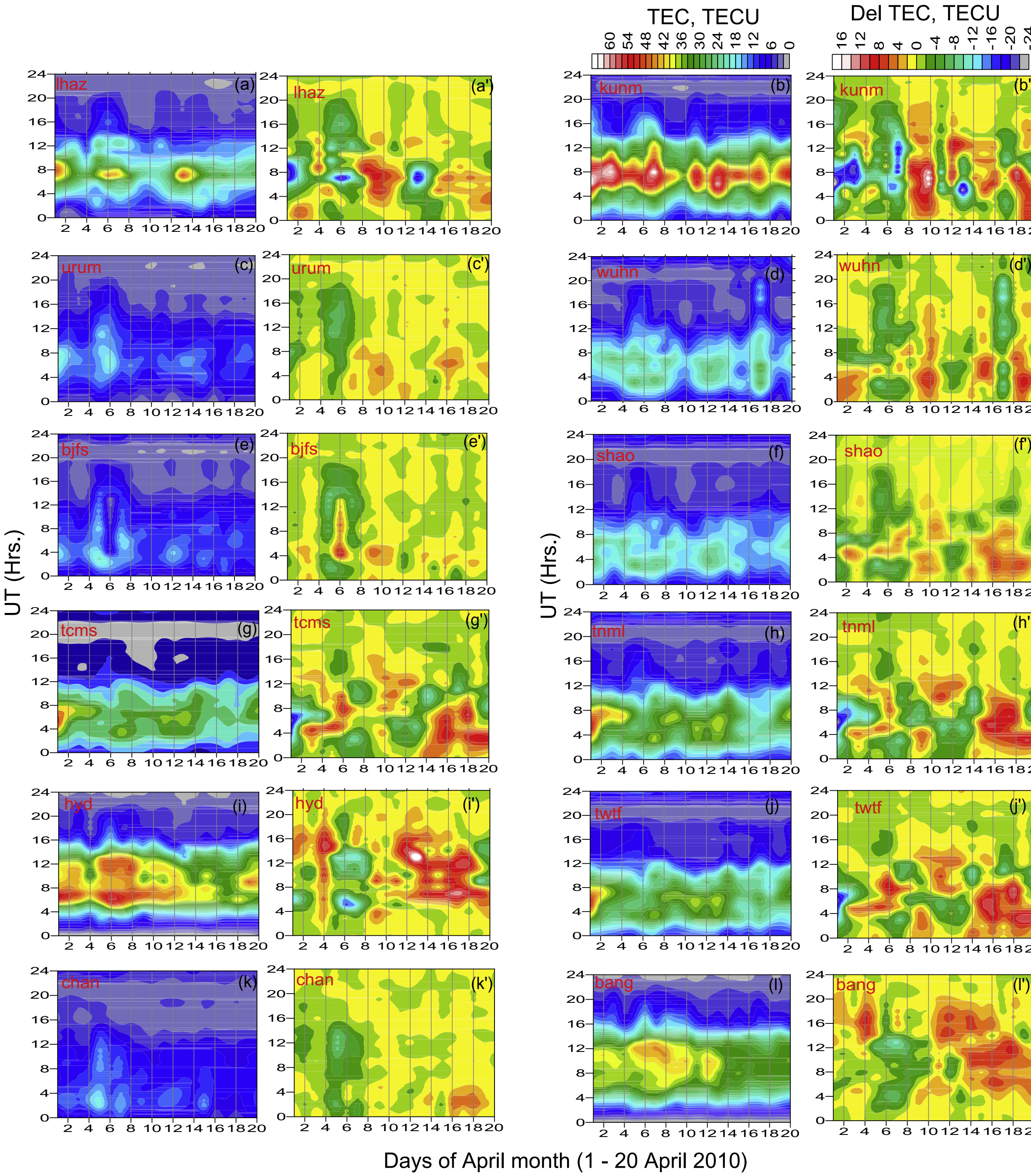

Fig. 3. Contour plots for the observed TEC (first and third column) and deviations of observed TEC from the median values (second & fourth column) for 1–20 April with respect to UT for each station. The stations are arranged with increase in the distance from the epicenter.

is higher through-out the day over the low-latitude (⩽30 deg) stations (lhaz, kunm, tcms, tnml, twtf, hyd and bang) whereas at other higher mid-latitude stations (urum, wuhn, bjfs, shao and chan) the response is weaker showing a latitudinal response of production processes of electrons in the ionosphere. On 1 Apr, higher TEC is observed during noon-time which can be explained as due to the higher production rate of electrons due to higher solar flux ($\sim 21 \times 10^9$ ph/cm^2/s).

The higher TEC is also observed during 5–7 April at all stations with maximum over hyd station (∼60 TECU) which lies near the peak of ionospheric equatorial ionization anomaly (EIA) region. The postsunset enhancement (around 1800 LT, ∼50 TECU) is also observed over same station, hyd. Recently, Aggarwal et al. (2013) also observed higher TEC at the anomaly station, Rajkot (geog. 22.29°N, 70.74°E), India during a moderate storm of 7–8 May 2005 and found associated with the pre-reversal enhancement of the electric field during evening hours. These changes in TEC in our Fig. 3 may be attributed to the storm period (Fig. 2) of 5–7 Apr (Dst ~ −81 nT). During geomagnetic storms, strong electric fields and currents are transmitted between the magnetosphere and the high-latitude ionosphere, producing enhanced Joule heating and auroral particle precipitation in the auroral region. The conductivity of the ionosphere gets increased, neutral winds are accelerated, the thermosphere is heated and its composition is altered, and ionospheric plasma convection is intensified and highly distorted. The perturbed neutral winds and composition propagate equatorward, creating ionospheric and thermospheric disturbances over the entire globe (e.g., Prolss, 1995).

Another increase in TEC is observed on 13 April (EQ day) over all the stations but the magnitudes are different being higher at lower-latitude station than over mid-latitude stations. These changes may again be attributed to the effects of moderate storm period (Dst ~ −67 nT) which occurred on 12 April (Fig. 2). The Del TEC also shows quantitatively the changes in TEC which occurred during the conditions of magnetic storm activity. The enhancements as well as decrements in TEC are highly variable for a few hours on all days for different stations with highest del TEC (~14 TECU, decrease in obs TEC) over hyd (on 13 Apr) and kunm (on 10 April) and lowest (increase in obs TEC) up to ~22 TECU over lhaz (on 1 April) and kunm (on 1 and 2 April) stations respectively.

To examine the anomalies in the ionosphere which may have occurred during the earthquake, we plotted the diurnal variability of observed TEC (Obs TEC), median (M), LQ and UQ as described in the 'data-analysis' section. Here in Fig. 4, the observations obtained from one of the station, lhaz is shown which lies in the radius of preparation zone of EQ. The deviations from the LB and UB (LB-Obs TEC and Obs TEC-UB) are also shown in the lower panels. Here the letter 'A' ('a') denotes the anomalous enhancement (depletion) in Obs TEC from the UB (LB) continuously for more than 7–8 h. From the figure, it is clear that on some days the Obs TEC lies between LQ and UQ whereas on other days it is either higher or lower than quartiles. Here the days 1, 2, 5, 6, 7, 10 and 16 are exhibiting anomalous features. As said before also, on 1 April the solar flux is higher and 5–7 are disturbed due to storm. On 10 Apr, the Obs TEC is lower than LB for 7 h, exhibiting anomalous signal in ionosphere. On 13 April also the TEC is higher which could be effect of moderate storm of 12 April but it was not anomalous as it was high only for few hours (<7 h). On 16 April, the difference is extremely small (<1 TECU). In the same manner, we examined the variability of Obs TEC and its deviation from the LB and UB for each station for 1–20 April 2010 (not shown as separate Figure).

To examine the enhancements and depletions in obs TEC quantitatively, the Fig. 5 is obtained showing the hourly deviations of Obs TEC from UB (Obs-UB) and LB (LB-Obs) as obtained from each station before, during and after EQ respectively. Though positive values of (LB-Obs) shows a depletions in Obs TEC, we only made it negative just to represent as depletions on plots (i.e. -(LB-Obs)). The maximum increase in Obs TEC w.r.t UB is up to ~20 TECU found over tcms and tnml stations. During 5–8 April, the enhancement is observed over all stations (up to ~12 TECU over hyd). The maximum depletion (~16 TECU) is observed on the day of EQ over hyd but it is only for 1 h and on other days, it is less than 8 TECU.

From Fig. 5, we could only obtain quantitative information about the deviations from the UB and LB but not the real anomalistic on each day. To examine it, we obtained the number of counts (number of anomalies detected on

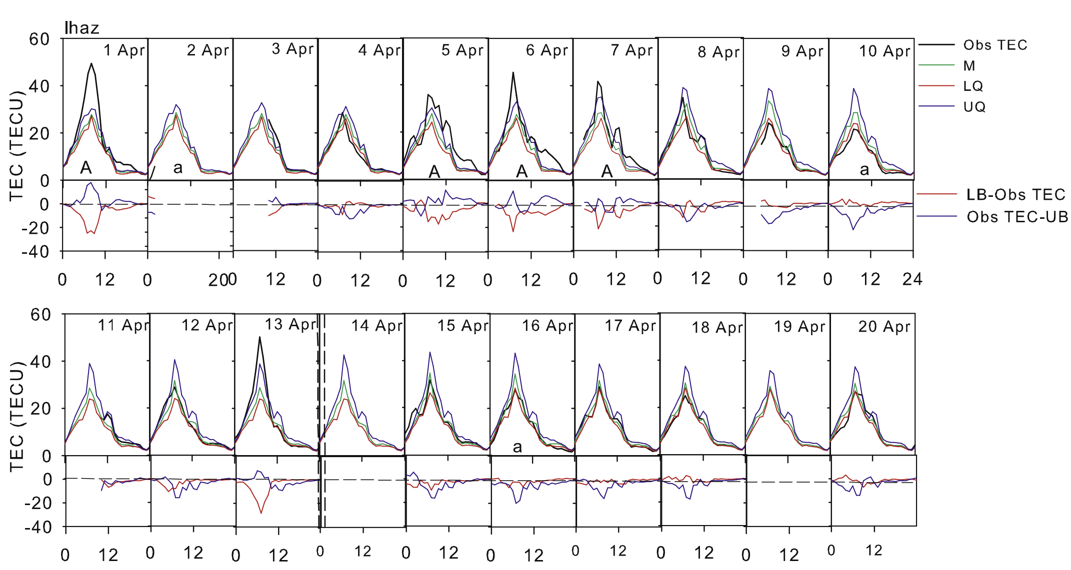

Fig. 4. Diurnal variation of observed TEC, Median (M), lower and upper quartiles (LQ & UQ) respectively on each day over LHAZ station. The lower panels show the variation in the LB-obs TEC and obsTEC-UB with UT.

each day) which shows the continuous enhancement or depletions in the TEC values from UB and LB respectively. Here the Fig. 6 represents the anomalous counts (>6) in UB and LB. It may be seen from figure that 11–12 days and 6–8 days before the EQ, the TEC has enhanced (lower panel) which is contributed to the high solar activity and disturbed period in these days as discussed earlier. The equatorial-low latitude ionospheric stations (hyd and bang) exhibits depletions on 4 April, for ~16 h over hyd and 11 h over bang. One of the significant factor that affects the F region ionization at low latitudes is the strength of equatorial electrojet current, EEJ (Sethia et al. 1980; Aravindan and Iyer, 1990). The electron density in the equatorial and anomaly F region also gets affected by the variations in the strength of EIA and EEJ strength as both (EEJ and EIA) are governed by the dynamo electric fields. The complex behavior of ionosphere shows depletion for 10 h observed over bjfs on 6 Apr which is a mid latitude station. We found from Fig. 6, anomalous depletions in TEC (upper panel) observed 3–4 days before the EQ in the ionosphere over nearby stations: lhaz, kunm, urum and wuhn consecutively for ~7–10 h. The ionospheric anomalous changes are firstly observed over wuhn (~0800–1600 UT) during afternoon to midnight hours which is ~1700 km away from the epicenter. And 6 h later the anomalous changes in TEC are observed over the near-by stations to the epicentre (lhaz, kunm, urum) in the nighttime (~1500–2300 UT, ~2100–0500 LT).

To summarize our findings, we represented the anomalies in Fig. 7 showing the distribution of abnormalities found in the ionosphere with the varying distance from the epicenter before the EQ event. We found the consecutive depletions in TEC (up to ~6 TECU) for many hours (Fig. 6) ~3–4 days before the EQ (10 April) in up to ~1700 km distant ionosphere from the epicenter. The enhancements in Obs TEC may not be attributed to the seismo-ionospheric anomalies as few days before was a moderate storm in the background.

However it is rather difficult to confirm causal relationships of the observed negative anomalies with pre-earthquakes phenomena, since these anomalies, apart from the space weather and forcing from above, can be caused by forcing from below by thermosphere, atmospheric meteorology- driven influences, tides, gravity and

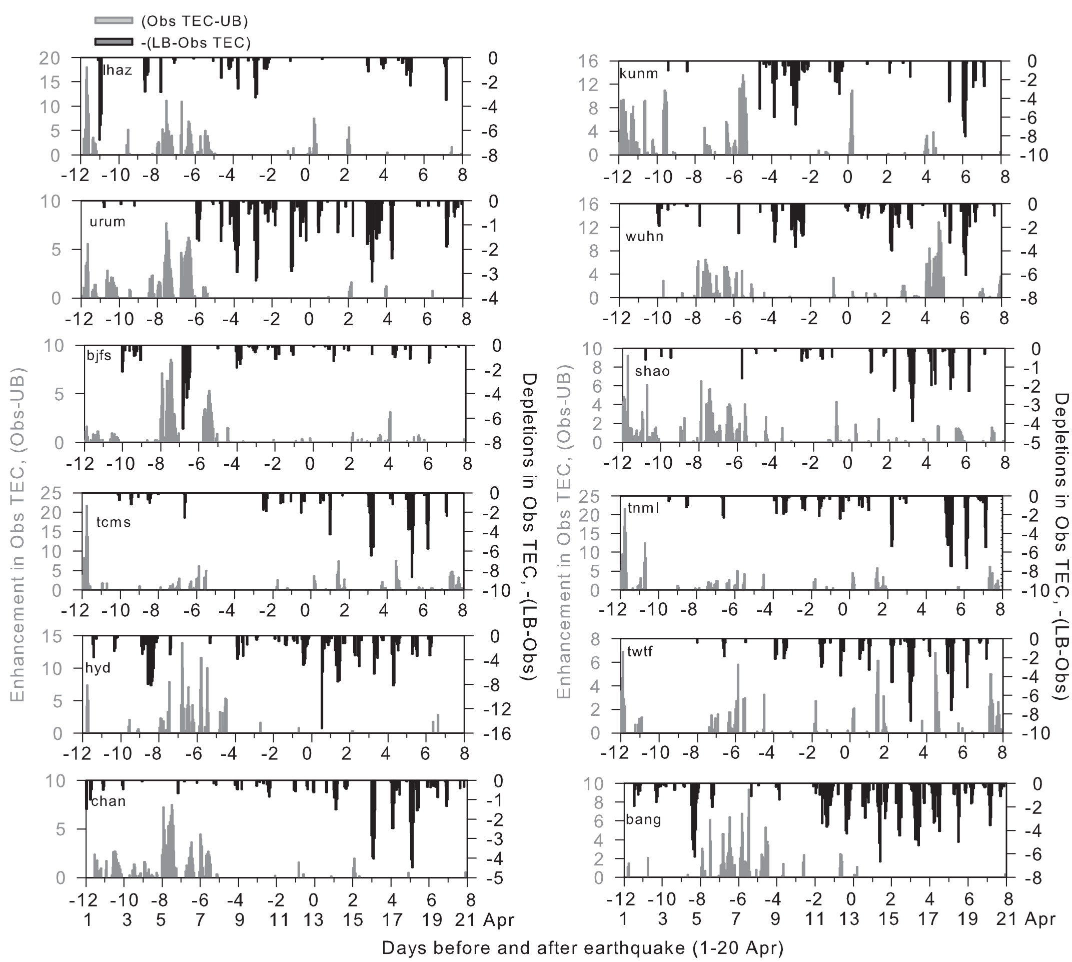

Fig. 5. Anomalous enhancements (left *Y*-axis) and decrements (right *Y*-axis) in the Obs TEC obtained from the deviations of Obs TEC from UB and LB on each day over all stations respectively. Note: Scale on y-axis is not same for each curve.

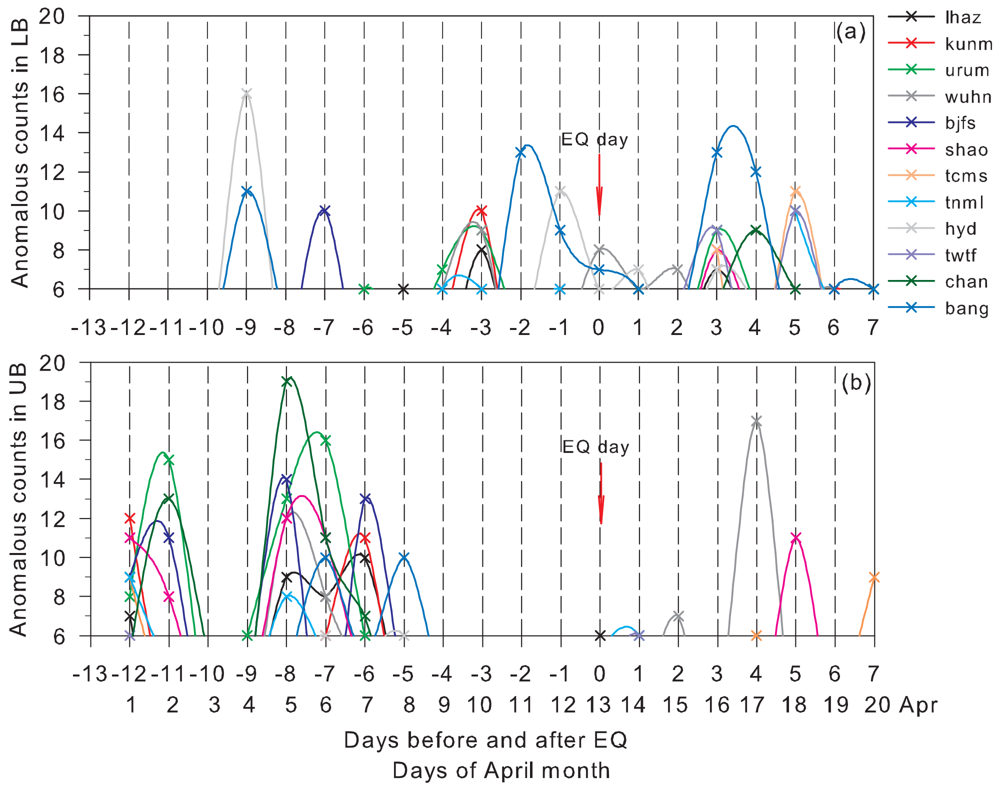

Fig. 6. Representation of the number of anomalous counts (>6) obtained in (a) LB-Obs and (b) Obs-UB from each station respectively. The upper (lower) plot shows the consecutive depletions (enhancement) in obs TEC. Here arrow shows the day when EQ occurred.

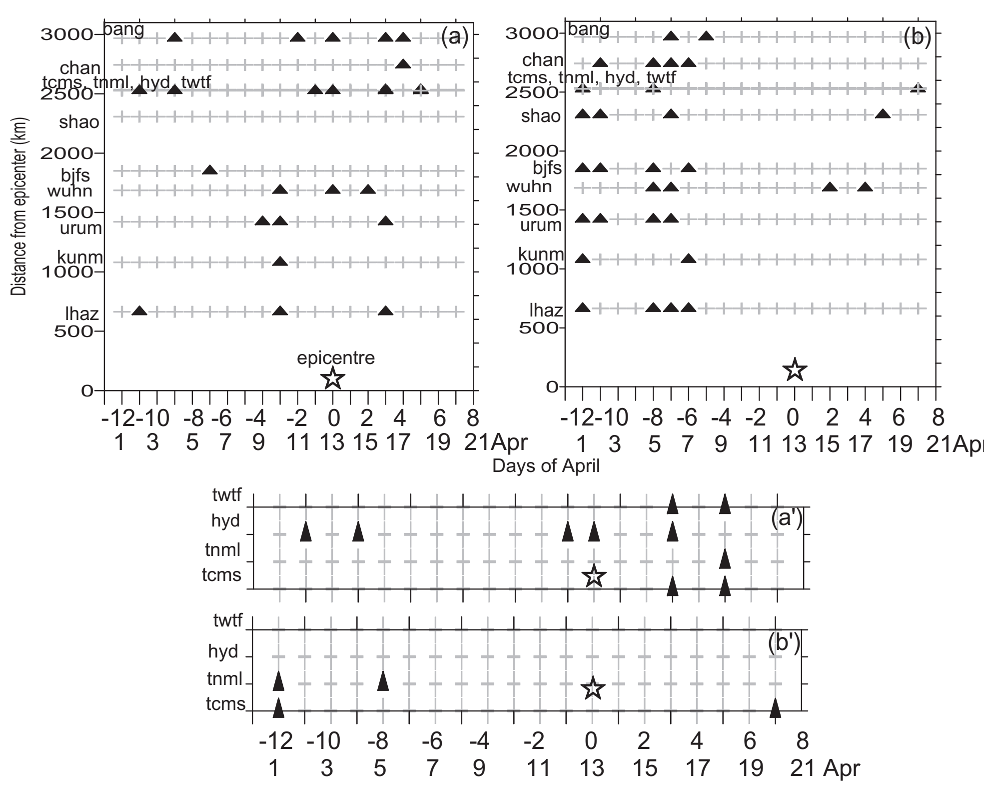

Fig. 7. Represents the anomalous days in (a) LB-Obs (depletions) and (b) Obs-UB (enhancement) with respect to the distance from the epicenter (shown by star) Here triangle shows the anomalous and plus sign, non-anomalous day. The bottom two plots shows the anomalous days (depletions: (a') & enhancement: (b')) in the enlarged form for very closed-by stations (tcms, tnml, hyd and twtf) to the epicenter to get a clear picture from each station.

planetary waves, etc. Modifications in atmospheric dynamics during magnetic storms take place through various processes like generation of equatorward neutral wind due to heating of high latitude thermosphere, prompt penetration of high latitude electric field (PPEF) to lower latitudes, and development of disturbances in the dynamo electric field (DDE) (Forbes, 1989; Abdu et al. 2006, 2012). Therefore, when an earthquake occurs during a magnetic storm, the ionosphere is influenced by (i) electric fields originated at the magnetosphere, (ii) the disturbed dynamo field and (iii) electric field of EQ preparatory sources. Thus a complexity increases when an earthquake occurs during a storm period making it rather difficult to claim the connection of the anomalies with the earth quakes. The explanation for anomalies observed on the two periods (5–7 April and 12–13 Apr) is in question and it seems is due to moderate magnetic storms.

Various previous scientists have also observed the anomalies appearing in electron densities of the ionospheric F region a few days before for some strong earthquake events (Pulinets, 1998; Pulinets et al. 2000, 2005; Liu et al. 2000, 2001) which is in agreement with our observations. Liu et al. 2000 and Liu et al. 2001 by exploring the ionospheric plasma frequency (or electron densities) recorded by a local ionosonde found significantly decrease in the critical frequency of the F2 layer (foF2) a few days prior to most of the earthquakes ($M > 6$) in the Taiwan area between 1994–1999. We found a decrease in TEC (<6 TECU) for more than 6 h 3–4 days prior to the earthquake at near-by stations (<1700 km). The anomalous ionospheric disturbances before some strong earthquakes of different seismic regions have been registered using GPS-TEC in the recent years. Liu et al. (2001) found movement of the equatorial anomaly crest towards the equator and significantly decrease in TEC around the epicenter during 1200–1700 LT, 1, 3, and 4 days before Taiwan Mw 7.7 Chi-Chi earthquake of 21 Sep 1999. Relative to the median of previous 15 days before Chi-Chi earthquake, the most severely decreasing region appeared about a radius of 100–200 km from the epicenter. Trigunait et al. (2004) have also shown the decrease of VTEC in the afternoon–evening sector, 1 and 5 days before Mw 7.6 Bhuj earthquake of 26 January, 2001, India. Liu et al. (2004a,b, 2010b) reported significant decreases in the GPS-TEC which appeared in the afternoon and evening periods within 1–6 days before earthquakes in Taiwan. Based on limited events, Liu et al. (2009) showed anomalous decreases of the TEC appearing in the afternoon or evening period 3–5 days before the large earthquakes in China. Liu et al. (2010a) found TEC anomalous decrease 1–8 day before large earthquakes in Indonesia. In contrast, Pulinets et al. (2006) reported the anomalous increment of TEC (>50% relative to the monthly mean) appeared 2–3 days before the Mw 7.8 Colima earthquake of 21 Jan 2003. Zakharenkova et al. (2006) observed modification of the equatorial anomaly occurred a few days before the 26 December 2004 Indonesian earthquake. A positive effect was observed in the daytime enhancing the equatorial anomaly (20 TECU, 50–60%) for 2 days prior to the event. Whereas in previous days, during the evening and night hours a double crest structure with a trough near the epicenter is observed. They assumed that anomalous electric field generated in the earthquake preparation zone could cause a near-natural "fountain effect" phenomenon and might be a possible cause of the observed ionospheric anomaly. Xiong et al. (2012) also studied the anomalies in ionospheric VTEC during the same EQ (of 13 Apr 2010) and found increase in TEC above the upper bound over the epicenter vicinity on 1 and 5 Apr, 2010. According to them, the enhancement on 5 April is related with the high geomagnetic activity. On 1 April, the geomagnetic activity was high for 3 h and they seem doubtful also because the anomalies appeared 12 days before the EQ, not 0–6 days as reported previously by Pulinets and Boyarchuk (2004) and Liu et al. (2004a, 2006). We also found such an anomalous increase on 1 Apr over many stations: lhaz, kunm, urum, bjfs, shao, tcms and tnml. But we are doubtful about it as the solar activity was also higher which may lead to higher production of electrons. Zhu et al. (2012) found a dynamic variability of the gravity field reflecting its evolution prior to and during this EQ. The gravity measurements near its epicenter became as high as 80×10^{-8} m/s^2. This EQ occurred in an anomalous area of gravity variation (associated with the accumulation of energy) and the associated steep gravity gradient, which supported the fracturing of it. Recently, Zhang et al. (2014) observed the anomalous increases in ionospheric parameters: foF2 from ionosonde, GPS-TEC and O^+ density by Demeter satellite on a day before the EQ.

Now, the question arises how the variability in the plasma (electrons, TEC) may occur in the ionosphere few days before the earthquake. Although, the exact mechanism of the lithosphere-ionosphere coupling is still not known, possible explanations have been advanced by many workers in terms of $E \times B$ drift mechanism where the electric field (E) triggered by an earthquake preparatory process penetrates the ionosphere and, in the presence of local magnetic field (B), causes upward or downward movement of the ionization depending upon the direction of the electric field (Devi et al. 2008). In addition to the electric field generation mechanism mentioned as above, more convincing mechanism has been proposed by some workers recently. Another proposed possible mechanism is the generation of acoustic gravity waves (AGWs) in the ionosphere before strong earthquakes. According to it, the AGWs generation occurs due to non-stationary Joule heating of a local region of the ionosphere above the epicentral zone of an imminent earthquake (Hegai et al. 1997, 2006). The AGWs play an important role for the interpretation of a large number of physical phenomena in the troposphere, and for the dynamics of the ionospheric plasma (Hines, 1960). Then the question remains to be answered about the mechanism of the electric field generation from the earthquake region. It is believed that these undetermined seismic-ionospheric anomalies may have a close relationship with the enhanced emission of infrared radiations from the epicenters. The one possibility for these pre-earthquake ionospheric anomalies could be strong atmospheric electric fields generated on, or near, the ground surface during pre-seismic periods. Such an atmospheric electric field may be caused by ions generated from radon emissions. The increased radon emanation from active faults and cracks before earthquakes can ionize the near ground atmosphere producing a large vertical electric field at the earth's surface (Pulinets and Boyarchuk, 2004). It was also pointed out by Freund (2000) that positively charged holes, associated with microfracturing prior to earthquakes, diffuse from the focal zone to the ground surface. Kim and Hegai (1999) and Pulinets et al. (2000) through a quasi-electrostatic model of atmosphere-thermo sphere-ionosphere coupling showed that a strong vertical electric field on the Earth's surface could penetrate into the ionosphere and alter its dynamics and electron density distribution prior to the earthquake onset. Their results estimated that a vertical electric field of $\sim$1 kV/m at the ground surface could produce a horizontal electric field of $\sim$1 mV/m at ionospheric heights. But, recently Xu et al. (2015) considering the effect of radon emanation on atmospheric conductivity solved numerically the electric potential equation in the presence of a vertical electric field of 1 kV/m on the ground. Their results showed that radon emanation can strengthen atmospheric conductivity resulting in the increased electric field by about 60% in the daytime ionosphere. But the resulting electric field in the ionosphere is weaker (only about 0.3 μV/m), implying the penetration of vertical electric field of 1 kV/m in the seismic area unlikely to produce daytime ionospheric anomalies before earthquakes. Denisenko et al. (2008) investigated the influence of the ionospheric conductivity on the electrostatic field penetration from the earth's surface into the ionosphere. They showed that the magnitude of the ionospheric electric field penetrated from the ground is inversely proportional to the value of the ionopheric Pedersen conductance. Hence the typical value in day-time is about hundred times lesser than in night-time. But still the penetrated electric field is not enough in the frame of the model of electro conductivity for a measurable disturbance of the ionospheric parameters as suggested by Denisenko et al. (2013) and hence study of other physical mechanisms may be needed to explain the lithospheric influence on the ionosphere.

Although many researchers reported the existence of pre-earthquake ionospheric anomalies and discussed the possible origins, the coupling mechanisms among the lithosphere, atmosphere and ionosphere are still not fully understood. The present study is focused only on demonstrating the ionospheric variability characteristics before the main shock of seismic event of 13 Apr. Since the magnetic storms mentioned above are unlikely to cause anomalous depletions in TEC occurred before the days of storm (on 10 Apr). We can believe that these may be produced as a precursor to the earthquake.

In conclusion, the anomalous depletion of the ionospheric TEC over near-by stations, lhaz, kunm, urum and wuhn 3–4 days prior to the strong earthquakes of China is unique. In the view of the near Earth–space environment, it was unlikely to be caused by the geomagnetic activities. Our results show that the dynamo electric field of the ionospheric regions might have been perturbed by seismo-electric signals generated around the epicenter during the earthquake preparation period. The spatial distribution of the anomalies was very local, which probably indicates association with seismo-ionospheric coupling processes. However, for elucidation of this kind of seismo-ionospheric effect, further investigation is required. Our future work will be to examine the variability of other plasma and neutral parameters in the ionosphere using higher number of events to understand the seismo-ionosphere coupling.

Acknowledgement

MA is grateful to the Department of Science and Technology (DST), India for providing the Ramanujan Fellowship to carry out the work. She is grateful to Prof. D.S Ramesh, Director of IIG, Mumbai for providing the hosting facilities at the Institute. She is also thankful to Dr. Gopi Seemala of IIG, Mumbai for useful discussions and sharing the software to analyze the GPS data from IGS stations. The GPS data collected from various IGS stations, OMNI website for geomagnetic and interplanetary data, the CELIAS/SEM experiment on SOHO spacecraft for EUV fluxes and the USGS community for sharing the earthquake characteristics are also highly acknowledged for making the data available. The author is grateful to the reviewers for their corrections, comments and suggestions in improving the manuscript.

References

Abdu, M.A., de Souza, J.R., Sobral, J.H.A., Batista, I.S., 2006. Magnetic storm associated disturbance dynamo effects in the low and equatorial latitude ionosphere. recurrent magnetic storms: corotating solar wind streams. In: Tsurutani, Bruce, McPherron, Robert, Gonzalez, Walter, Lu, Gang, Sobral, José H.A., Gopalswamy, Natchimuthukonar (Eds.), Geophysical Monograph, 167. AGU Books Board, AGU, Washington, DC USA, p. 283, ISBN-13: 978-0-87590-432-0.

Abdu, M.A., Batista, I.S., Bertoni, F., Reinisch, B.W., Kherani, E.A., Sobral, J.H.A., 2012. Equatorial ionosphere responses to two magnetic storms of moderate intensity from conjugate point observations in Brazil. J. Geophys. Res. 117 (A5), CiteID A05321.

Afraimovich, E.L., Astafyeva, E.I., 2008. TEC anomalies local TEC changes prior to earthquakes or TEC response to solar and geomagnetic activity changes? Earth Planets Space 60, 961–966.

Aggarwal, M., Joshi, H.P., Iyer, K.N., Kwak, Y.S., 2013. Response of the EIA ionosphere to the 7–8 May 2005 geomagnetic storm. Adv. Space Res. 52 (4), 591–603.

Akhoondzadeh, M., Parrot, M., Saradjian, M.R., 2010. Electron and ion density variations before strong earthquakes ($M > 6.0$) using DEMETER and GPS data. Nat. Hazards Earth Syst. Sci. 10 (1), 7–18.

Allen, J., 2010. The galaxy 15 anomaly: another satellite in the wrong place at a critical time. Space Weather 8, S06008. http://dx.doi.org/10.1029/2010SW000588.

Aravindan, P., Iyer, K.N., 1990. Day-to-day variability in ionospheric electron content at low latitudes. Planet. Space Sci., 0032-0633 38, 743–750.

Astafyeva, E., Heki, K., 2011. Vertical TEC over seismically active region during low solar activity. J. Atmos. Sol. Terr. Phys. 73 (13), 1643–1652.

Astafyeva, E., Shalimov, S., Olshanskaya, E., Lognonné, P., 2013. Ionospheric response to earthquakes of different magnitudes: larger quakes perturb the ionosphere stronger and longer. Geophys. Res. Lett. 40 (9), 1675–1681.

Calais, E., Minster, J.B., 1995. GPS detection of ionospheric perturbations following the January 17, 1994, northridge earthquake. Geophys. Res. Lett., 0094-8276 22 (9), 1045–1048.

Devi, M., Barbara, A.K., Depueva, A., Depuev, V., 2008. Preliminary results of TEC measurements in Guwahati, India. Adv. Space Res. 42, 753–756.

Denisenko, V.V., Boudjada, M.Y., Horn, M., Pomozov, E.V., Biernat, H.K., Schwingenschuh, K., Lammer, H., Prattes, G., Cristea, E., 2008. Ionospheric conductivity effects on electrostatic field penetration into the ionosphere. Nat. Hazards Earth Syst. Sci. 8, 1009–1017.

Denisenko, V.V., Ampferer, M., Pomozov, E.V., Kitaev, A.V., Hausleitner, W., Stangl, G., Biernat, H.K., 2013. On electric field penetration from ground into the ionosphere. J. Atmos. Sol. Terr. Phys. 102, 341–353.

Dobrovolsky, I.P., Zubkov, S.I., Miachkin, V.I., 1979. Estimation of the size of earthquake preparation zones. Pure Appl. Geophys. 117, 1025–1044.

Forbes, J.M., 1989. Evidence for the equatorward penetration of electric fields, winds, and compositional effects in the Asian/Pacific sector during the September 17-24, 1984 ETS interval. J. Geophys. Res., 0148-0227 94, 16999–17007.

Freund, F., 2000. Toward a unified solid state theory for pre-earthquake signals. Acta Geophys. 58 (5), 719–766.

Gokhberg, M.B., Morgounov, V.A., Yoshino, T., Tomizawa, I., 1982. Experimental measurement of electromagnetic emissions possibly related to earthquakes in Japan. J. Geophys. Res. Solid Earth 87 (B9), 7824–7828.

Gokhberg, M.B., Pilipenko, V.A., Pokhotelov, O.A., 1983. Observations from a satellite of electromagnetic radiation above the region of an earthquake in preparation. Doklady AN SSSR (Reports to the USSR Acad. Sci.). 268, 56–58.

Gokhberg, M.B., Nekrasov, A.K., Shalimov, S.L., 1994. A new approach to the problem of the lithosphere-ionosphere coupling before the earthquakes. In: Hayakawa, M., Fujinawa, Y. (Eds.), Electromagnetic Phenomena Related to Earthquake Prediction. Terra Sci. Publ. Co., Tokyo, pp. 619–625.

Hayakawa, M., Fujinawa, Y. (Eds.), 1994. Electromagnetic Phenomena Related to Earth-quake Prediction. TERRAPUB, Tokyo (pp. 677).

Hayakawa, M., Molchanov, O.A. (Eds.), 2002. Seismo Electromagnetics Lithosphere-Atmosphere-Ionosphere Coupling. TERRAPUB, Tokyo, p. 477.

Hegai, V.V., Kim, V.P., Nikiforova, L.L., 1997. A possible generation mechanism of acoustic-gravity waves in the ionosphere before strong earthquakes. J. Earthquake Pred. Res. 6, 584–589.

Hegai, V.V., Kim, V.P., Liu, J.Y., 2006. The ionospheric effect of atmospheric gravity waves excited prior to strong earthquake. Adv. Space Res. 37, 653–659.

Hines, C.O., 1960. Internal atmospheric gravity waves at ionospheric heights. Can. J. Phys. 38, 1441–1481.

Kim, V.P., Hegai, V.V., 1999. A possible presage of strong earthquakes in the night-time mid-latitude F2 region ionosphere. In: Hayakawa, M. (Ed.), Atmospheric and Ionospheric Electromagnetic Phenomena Associated with Earthquakes. Terra Science Publishing Co., Tokyo, pp. 619–627.

Kinrade, J., Mitchell, C.N., Yin, P., Smith, N., Jarvis, M.J., Maxfield, D.J., Rose, M.C., Bust, G.S., Weatherwax, A.T., 2012. Ionospheric scintillation over Antarctica during the storm of 5–6 April 2010. J. Geophys. Res. 117 (A5), CiteID A05304.

Klobuchar, J., 1986. Design and characteristics of the GPS ionospheric timedelay algorithm for single frequency users. In: Proceedings of PLANS'86 – Position Location and Navigation Symposium, 4–7 November. Las Vegas, Nevada, pp. 280–286.

Klotz, S., Johnson, N.L. (Eds.), 1983. Encyclopedia of Statistical Sciences. John Wiley and Sons.

Liu, J.Y., Chen, Y.I., Pulinets, S.A., Tsai, Y.B., Chuo, Y.J., 2000. Seismo-ionospheric signatures prior to $M > 6.0$ Taiwan earthquakes. Geophys. Res. Lett. 27, 3113–3116.

Liu, J.Y., Chen, Y.I., Chuo, Y.J., Tsai, H.F., 2001. Variations of ionospheric total electron content during the Chi-Chi earthquake. Geophys. Res. Lett. 28, 1383–1386.

Liu, J.Y., Chuo, Y.J., Shan, S.J., Tsai, Y.B., Chen, Y.I., Pulinets, S.A., Yu, S.B., 2004a. Pre-earthquake ionospheric anomalies registered by continuous GPS TEC measurements. Ann. Geophys. 22, 1585–1593.

Liu, J.Y., Chen, Y.I., Jhuang, H.K., Lin, Y.H., 2004b. Ionospheric foF2 and TEC anomalous days associated with $M >= 5.0$ earthquakes in Taiwan during 1997–1999. Terr. Atmos. Oceanic Sci. 15, 371–383.

Liu, J.Y., Chen, Y.I., Chuo, Y.J., Chen, C.S., 2006. A statistical investigation of pre-earthquake ionospheric anomaly. J. Geophys. Res. 111 (A5), CiteID A05304.

Liu, J.Y., Chen, Y.I., Chen, C.H., Liu, C.Y., Chen, C.Y., Nishihashi, M., Li, J.Z., Xia, Y.Q., Oyama, K.I., Hattori, K., Lin, C.H., 2009. Seismoionospheric GPS total electron content anomalies observed before the 12 May 2008 Mw7.9 Wenchuan earthquake. J. Geophys. Res. 114, A04320. http://dx.doi.org/10.1029/2008JA013698.

Liu, J.Y., Chen, Y.I., Chen, C.H., Hattori, K., 2010a. Temporal and spatial anomalies in the ionospheric GPS total electron content observed before the 26 December 2004 M9.3 Sumatra-Andaman earthquake. J. Geophys. Res. 115, A09312. http://dx.doi.org/10.1029/2010JA015313.

Liu, J.Y., Chen, C.H., Chen, Y.I., Yang, W.H., Oyama, K.I., Kuo, K.W., 2010b. A statistical study of ionospheric earthquake precursors monitored by using equatorial ionization anomaly of GPS TEC in Taiwan during 2001–2007. J. Asian Earth Sci. 39, 76–80.

Molchanov, O.A., Hayakawa, M., 2001. VLF monitoring of atmosphere–ionosphere boundary as a tool to study planetary waves evolution and seismic influence. Phys. Chem. Earth C 26, 453–458.

Parrot, M., Lefeuvre, F., 1985. Correlation between GOES VLF emissions and earthquakes. Ann. Geophys. 3, 733–748.

Plotkin, V.V., 2003. GPS detection of ionospheric perturbation before the 13 February 2001, El Salvador earthquake. Nat. Hazards Earth Syst. Sci. 3 (3/4), 249–253.

Prikryl, P., Spogli, L., Jayachandran, P.T., Kinrade, J., Mitchell, C.N., Ning, B., Li, G., Cilliers, P.J., Terkildsen, M., Danskin, D.W., Spanswick, E., Donovan, E., Weatherwax, A.T., Bristow, W.A., Alfonsi, L.De., Franceschi, G., Romano, V., Ngwira, C.M., Opperman, B.D.L., 2011. Interhemispheric comparison of GPS phase scintillation at high latitudes during the magnetic-cloud-induced geomagnetic storm of 5–7 April 2010. Ann. Geophys. 29, 2287–2304. http://dx.doi.org/10.5194/angeo-29-2287-2304.

Prolss, G.W., 1995. Ionospheric F region storms. In: Volland, H. (Ed.), Handbook of Atmospheric Electrodynamics. CRC Press, Boca Raton, pp. 195–248.

Pulinets, S.A., Legen'ka, A.D., Alekeseev, V.A., 1994. Pre earthquake ionospheric effects and their possible mechanisms. In: Dusty and Dirty Plasmas. Noise and Chaos in Space and in Laboratory. Plenum Publishing, New York, pp. 545–557.

Pulinets, S.A., 1998. Seismic activity as a source of the ionospheric variability. Adv. Space Res. 22 (6), 903–906.

Pulinets, S.A., Boyarchuk, K.A., 2004. Ionospheric Precursors of Earthquakes. Springer, Berlin, Germany, 315.

Pulinets, S.A., Boyarchuk, K.A., Hegai, V.V., Kim, V.P., Lomonosov, A.M., 2000. Quasielectrostatic model of atmosphere-thermosphere-ionosphere coupling. Adv. Space Res. 26 (8), 1209–1218.

Pulinets, S.A., Boyarchuk, K.A., Hegai, V.V., Karelin, A.V., 2002. Conception and model of seismo-ionosphere magnetosphere coupling.

In: Hayakawa, M., Molchanov, O.A. (Eds.), Seismo-Electromagnetics: Lithosphere-Atmosphere-Ionosphere Coupling. TERRAPUB, Tokyo, pp. 353–361.

Pulinets, S.A., Legen'ka, A.D., Gaivoronskaya, T.V., Depuev, V.K., 2003. Main phenomenological features of ionospheric precursors of strong earthquakes. J. Atmos. Sol. Terr. Phys. 65, 1337–1347.

Pulinets, S.A., Leyva Contreras, A., Bisiacchi-Giraldi, G., Ciraolo, L., 2005. Total electron content variations in the ionosphere before the colima, Mexico earthquake of 21 January 2003. Geofis. Int. 44 (4), 369-337.

Pulinets, S.A., Ouzounov, D., Ciraolo, L., Singh, R., Cervone, G., Leyva, A., Dunajecka, M., Karelin, A.V., Boyarchuk, K.A., Kotsarenko, A., 2006. Thermal, atmospheric and ionospheric anomalies around the time of the Colima M7.8 earthquake of 21 January 2003. Ann. Geophys. 24 (3), 835–849.

Pundhir, D., Singh, B., Singh, O.P., 2014. Anomalous TEC variations associated with the strong Pakistan-Iran border region earthquake of 16 April 2013 at a low latitude station Agra, India. Adv. Space Res. 53 (2), 226–232.

Ruzhin, Yu.Ya., Oraevsky, V.N., Shagimuratov, I.I., Sinelnikov, V.M., 2002. Ionospheric precursors of earthquakes revealed from GPS data and their connection with "sea-land" boundary. In: Proc. 16th Wroclaw EMC Symposium, pp. 723–726.

Sharma, D.K., Bardhan, A., Rai, J., 2013. Ionospheric electron and ion temperatures response to seismic activity. Indian J. Radio Space Phys. 42, 18–26.

Sharma, K., Dabas, R.S., Sarkar, S.K., Das, R.M., Ravindran, S., Gwal, A.K., 2010. Anomalous enhancement of ionospheric F2 layer critical frequency and total electron content over low latitudes before three recent major earthquakes in China. J. Geophys. Res.: Space Phys. 115 (A11), CiteID A11313.

Sethia, G., Chandra, H., Deshpande, M.R., Rastogi, R.G., 1980. Radio beacon studies of equatorial electron content, In: Low latitude aeronomical processes. Proceedings of the Symposium, Bangalore, India, May 29-June 9, 1979, (A80–52226 23–46). Pergamon Press, Oxford and Elmsford, N.Y., p. 161–164.

Stein, S., Okal, E.A., 2005. Seismology: speed and size of the Sumatra earthquake. Nature 434 (7033), 581–582.

Trigunait, A., Parrot, M., Pulinets, S., Li, F., 2004. Variations of the ionospheric electron density during the Bhuj seismic event. Ann. Geophys. 22 (12), 4123–4131.

Tronin, A.A., Hayakawa, M., Molchanov, O.A., 2002. Thermal IR satellite data application for earthquake research in Japan and China. J. Geodyn. 33 (4), 519–534.

Xia, Y., Liu, J.Y.T., Cui, X., Li, J., Chen, W., Liu, C., 2011. Abnormal infrasound signals before 92 $M \geqq 7.0$ worldwide earthquakes during 2002–2008. J. Asian Earth Sci. 41 (4), 434–441.

Xiong, J., Zhou, Y.Y., Wu, Y., 2012. Ionospheric VTEC anomalies before Ms 7.1 Yushu earthquake. Geod. Geodyn. 2, 48–52.

Zakharenkova, I.E., Krankowski, A., Shagimuratov, I.I., 2006. Modification of the low-latitude ionosphere before the 26 December 2004 Indonesian earthquake. Nat. Hazards Earth Syst. Sci. 6 (5), 817–823.

Xu, T., Zhang, H., Hua, Y., Wua, J., 2015. Electric field penetration into the ionosphere in the presence of anomalous radon emanation. Adv. Space Res. 55, 2883–2888.

Zhang, X.M., Liu, J., Zhao, B.Q., Xu, T., Shen, X., Yao, L., 2014. Analysis on ionospheric perturbations before Yushu Earthquake. Chin. J. Space Sci. 34 (6), 822–829. http://dx.doi.org/10.11728/cjss2014.06.822.

Zhu, Y., Liu, F., Cao, J., Zhao, Y., 2012. Gravity changes before and after the 2010 Ms7.1 Yushu earthquake. Geod. Geodyn. 3 (4), 1–7.